JOURNAL OF MATERIALS SCIENCE 32 (1997) 123–128

Interaction between dislocations and precipitated water bubbles during high temperature creep of quartz

A. AYENSU
Department of Physics, University of Cape Coast, Cape Coast, Ghana

The modes of interaction between dislocations and precipitated water bubbles in quartz are discussed. It is shown that dislocations may be locally anchored by bubbles, but are able to break away under the action of applied stress. To escape, dislocations pinned by bubbles must bow to equilibrium curvature. It was observed that escape via thermal activation alone was not readily possible; however, unpinning of the dislocation through pipe diffusion was found to be possible if the dislocation could drag the bubbles under applied stress. This could result in very small strains leading to a microcreep rate linearly dependent on stress and independent of the concentration of bubbles.

1. Introduction

The mechanism of hydrolytic weakening of quartz has been attributed to the hydrolysis of strained Si–O bonds residing at dislocation cores [1, 2]. The corresponding Frank–Griggs expression for hydrolytic reaction is

$$\equiv \text{Si–O–Si} \equiv \; + \text{H}_2\text{O} \rightarrow \equiv \text{Si–O–H}\cdots\text{H–O–Si} \equiv$$

which is driven by the release of dislocation strain energy. The overall plasticity is therefore assumed to be associated with the scissioning of the SiO_4 tetrahedra, with molecular water acting as a plasticizer [3]. It is now accepted that high temperature deformation of quartz is associated with continuous precipitation of molecular water [4–12].

Irrespective of the validity of the atomic mechanisms for hydrolytic weakening reported [13–19], there remain the effects of dislocation–water bubble interactions on glide and climb of dislocations. It must be mentioned that the interaction of dislocations and bubbles, and the subsequent hardening of the crystal when water precipitates as bubbles, may be complicated by Peierls-Nabarro forces. Subsequently, an external force greater than the Peierls–Nabarro force must therefore be applied along a crystallographic direction if the dislocation is to move freely over considerable distances.

In this paper, the possible modes of dislocation–water bubble interactions and the mechanisms of accommodation that ensure large plastic flow by climb and glide will be discussed. The analysis will be likened to the theory of interaction of fission-gas bubbles with dislocations in irradiated nuclear materials [20–23], or to the dragging of unsaturated impurity clouds by dislocations [24]. A typical case of interest that will be considered is whereby a dislocation is pinned at two bubbles such that the glide and climb processes cause the dislocation to "bow" between two fixed positions.

2. Results

2.1. Deformation substructures

Transmission electron micrographs of synthetic quartz deformed at 800 °C are shown in Figs 1 and 2. The arrows point to precipitated water bubbles in a cloud of dislocations. The bubbles show up as the white contrasts in the bright field images. Some of the dislocations are pinned by bubbles and it is expected that the bubbles may impose a retarding effect on dislocation mobility because the precipitates remain fixed in the matrix.

A bubble therefore presents to a dislocation an area of crystal surface, so that the possibility of an image force attracting the dislocation to the bubble may exist. As a consequence of the interaction, the crystal will gain a quantity of energy equivalent to the line energy for a dislocation length equal to the bubble diameter. This energy has to be resupplied if the dislocation is to break free during subsequent deformation. By the same token, this energy will have to be supplied before the bubble can migrate during annealing in the absence of dislocation motion.

In Fig. 1, dislocations H–H′ and S–S′ are bound to water bubbles and must bow to significant curvature before unpinning can take place. Similarly, as shown in Fig. 2, dislocation X–X′ is bound to precipitated water bubbles Y and Y_1. The dislocation H–H′ in Fig. 1 is pinned at two bubbles, Q and Q_1 that are separated by a distance of ~ 0.5 μm; and in order to escape, the dislocation would have to adopt a curvature by looping process. If the elastic energy per unit length (or line tension) of the free dislocation is taken to be $\tau_o = 0.5\,\mu b^2$ (where μ is the shear modulus and

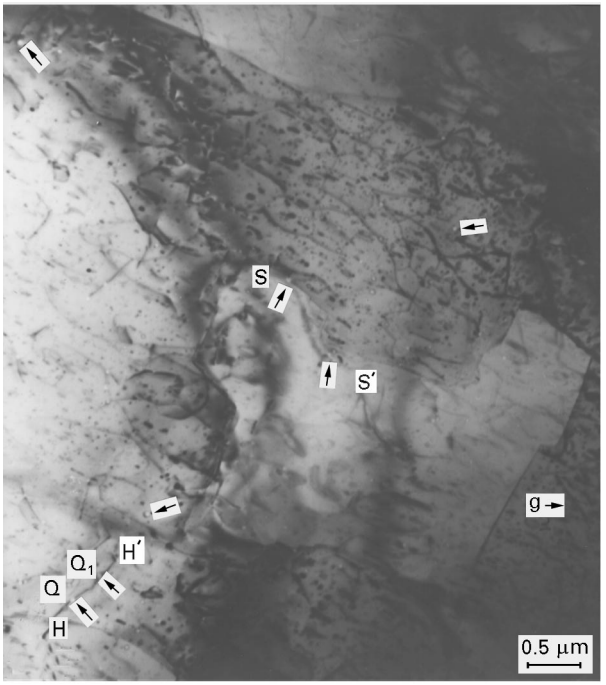

Figure 1 Dislocation structures (H–H′ and S–S′) in synthetic quartz after creep deformation at 800 °C. The arrows point to bubbles (e.g. Q and Q_1) of phase-separated water formed during post-deformation annealing. Foil plane $(1\,1\,\bar{2}\,0)$, diffracted beam $g = [1\,\bar{1}\,0\,1]$, 200 kV.

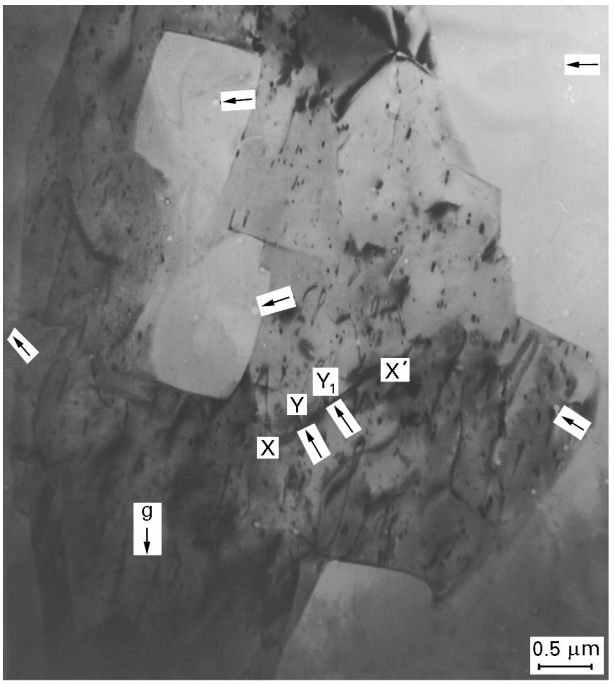

Figure 2 Phase-separated water, dislocations (X–X′) and Dauphiné twin boundaries (shown by contrast effect) in synthetic quartz deformed at 800 °C. The average water bubble diameter is 40.0 nm. Arrows point to phase-separated water bubbles. (e.g. Y and Y_1). Foil plane $(1\,1\,\bar{2}\,0)$, diffracted beam $g = [1\,\bar{1}\,0\,1]$, 200 kV.

b is the magnitude of the Burgers vector), then the energy of the dislocation line equivalent to the bubble diameter, δ, is $W = 0.5\,\mu b^2\delta$. For quartz, $\mu = 80$ GPa, $b = 0.586$ nm, $\delta = 40.0$ nm and the line tension is $\sim 1.4 \times 10^{-8}$ J m^{-1}. For a bubble of ~ 40.0 nm diameter, the corresponding force of attraction between a bubble and a dislocation is at least 0.4 N m^{-1}, and the total binding energy can be estimated to be $W = 6.4 \times 10^{-16}$ J. Despite this low force of attraction, movement of the dislocation by small stresses can be prevented by a hardening mechanism due to pinning and can also be prevented if diffusional processes are arrested.

Preferential precipitation of water bubbles on dislocations could be due to long range attraction to the dislocations by isolated bubbles or easier nucleation as dislocations can emit or absorb vacancies that are necessary to relax changes in volume due to precipitation.

To preserve the silicon–oxygen ratio, it is convenient to describe dislocation cores of SiO_4 tetrahedra in single and double helices of ***a*** and ***c*** channels, as shown in Fig. 3 [25], because diffusion can occur along the core of the dislocation. Therefore, hydrolytic weakening requires pipe diffusion of molecular water to the dislocation cores, as diffusion of water molecules through the channels would involve a much lower activation energy compared with lattice diffusion.

2.2. Thermal escape of pinned dislocations

If a dislocation is introduced into a quartz crystal of uniform concentration of bubbles of average value, C_o, the bubbles at a distance, λ, from the dislocation will be subjected to a force, $\boldsymbol{F} = -\text{grad}\ W$, that might draw the bubbles towards the dislocation with a drift velocity, $\boldsymbol{v} = D_B\boldsymbol{F}/kT$ (where D_B is the diffusion coefficient of the bubbles, k is the Boltzmann constant, T is the temperature and W is the binding energy).

As observed in Section 2.1., in the case of unsaturated bubble clouds, the dislocations may be considered to be pinned as illustrated in Fig. 4a. During the unpinning process, a length of dislocation, l, between two pinning points (A_2 A_3) bows out under an increasing stress, until the dislocation escapes from one pinning point as shown in Fig. 4b. If the pinning bubbles are more or less equally spaced, the stress concentrations at the neighbouring pinning bubbles are then sufficient to unpin them too; and, eventually, the whole loop (B_1B_2) is freed to bow out to sweep through an area, A. Fig. 4c therefore represents a stage of the unpinning process whereby between B_1B_2 there were many bubbles from which dislocations broke away, with B_1 and B_2 acting as the stronger pinning points or large bubble sites.

If ρ is the dislocation density, L is the distance between pinning points, ν is the atomic frequency and σ is the applied stress, the strain rate can be written as [26]

$$\dot{\varepsilon} = \frac{\rho}{L} bA\left(\nu\frac{b}{L}\right)\exp\left(\frac{-W + \sigma b^2 L}{kT}\right) \qquad (1)$$

and at thermal equilibrium, L is related to the binding energy by the equation [27]

$$\frac{L}{b} = C_o \exp\left(-\frac{W}{kT}\right) \qquad (2)$$

where C_o is the average bubble concentration and T is the temperature of the heat treatment during which the bubbles are formed.

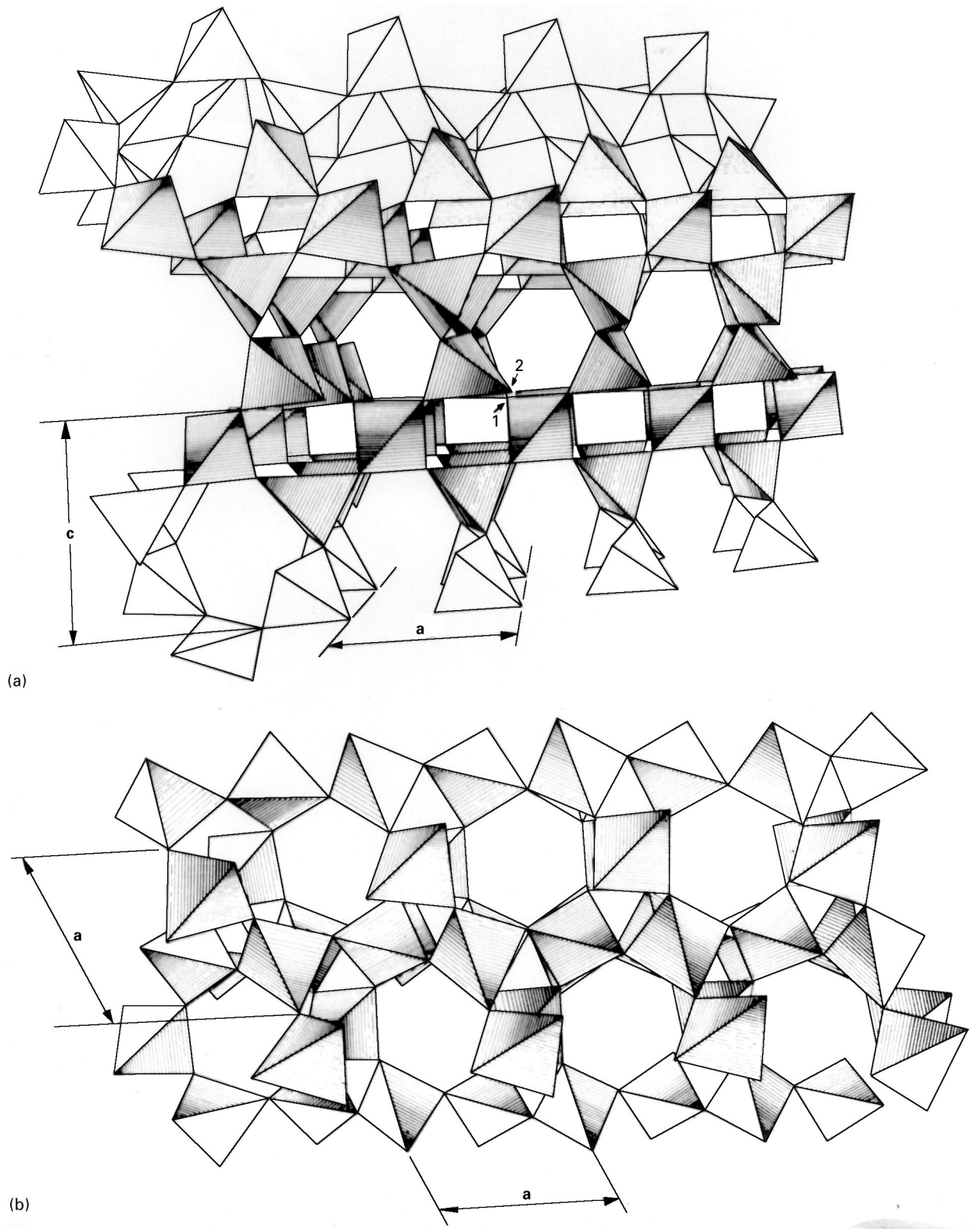

Figure 3 Structure of morphologically right-handed β-quartz ($P6_422$) viewed parallel to ***a*** in (a) and parallel to **c** in (b). In Fig. 3a, the numbers 1 and 2 represent the scissioning of SiO_4 tetrahedra.

As shown in Fig. 4c, if due to thermal agitation, kT, a length of the dislocation escapes under the action of stress, σ, at a curvature, $1/R = 2\sigma/\mu b$, the energy required to form this loop can be written as [26]

$$E = \left[\tau_o\theta - 2\tau\sin\left(\frac{\theta}{2}\right)\right]R - \sigma bA \qquad (3)$$

where τ_o is the line tension of the free dislocation, which is related to the line tension of the pinned dislocation, τ, by the equation

$$\tau = \tau_o - \left(C_1\frac{Wr}{b^2}\right) \qquad (4)$$

where the saturation concentration $C_1 = \frac{1}{2}$, r is the cylindrical region of saturation where the concentration

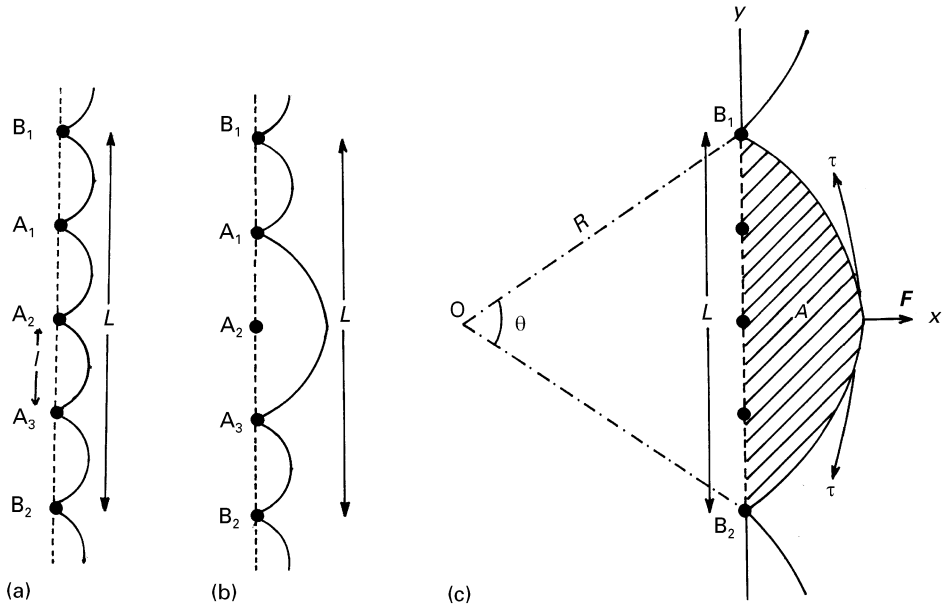

Figure 4 (a) Bowing-out of dislocation lines, (b) unpinning of dislocation lines, and (c) equilibrium curvature $1/R$, of a length L, of pinned dislocation under stress, where A_i and B_i are the pinning points, l is the length between two points, A is the area of unpinning, $\boldsymbol{F}$ the force acting in the x- and y-directions and τ the elastic energy per unit length, L of the pinned dislocation, and θ is the angle of curvature.

is of the order of C_1 and area, $A = \frac{1}{2}R^2(\theta - \sin\theta)$ is the shaded region in Fig. 4c.

The energy, E, passes through a maximum value, E_o, when $\tau_o = \tau\cos(\theta/2)$. For small angles, $\tau/\tau_o \approx 1$, and $L \approx 2R\sin(\theta/2) = (\mu b/\sigma)\sin(\theta/2)$. Substituting $\tau_o = 0.5\,\mu b^2$ in Equation 3 and applying binomial expansion, it can be deduced that the activation energy is

$$E_o = \tfrac{2}{3}\left(\frac{rL}{b^2}\right)WC_1 \tag{5}$$

and the corresponding length of the pinned dislocation is

$$L = 2\frac{\mu b}{\sigma}\left(C_1\frac{Wr}{\mu b^4}\right)^{1/2} \tag{6}$$

Substituting values of $L = 5\times10^{-7}$ m, $r = \delta = 4\times10^{-8}$ m, $b = 5.86\times10^{-10}$ m, $W = 6.4\times10^{-16}$ J, the numerical value of E_o is 3×10^{-11} J; which is a very large energy and will lead to a negligible rate of thermal escape. The alternative is to consider climb by a pipe diffusion mechanism.

However, if there is a possibility of thermal activated escape of dislocations from unsaturated bubbles, Equation 1 can be applied if, for small stress, the area swept by each free dislocation loop is given as $A = \sigma L^3/12\,\mu b$, and Equation 1 reduces to

$$\dot{\varepsilon} = \frac{\nu L C_o^2}{12\,\mu b}\,\sigma\exp\left(-\frac{W}{kT}\right) \tag{7}$$

after substituting $\rho L^2 = 1$ and Equation 2.

2.3. Dislocation climb by pipe diffusion

Fig. 4c illustrates a length of dislocation that is pinned at two ends by water bubbles and is subjected to a force, $\boldsymbol{F}$, due to the applied stress, σ. If the dislocation loop is mobile in the direction of $\boldsymbol{F}$, it will assume an equilibrium curvature, $1/R$, obtained by equating the force, $\tau_o d\theta$, of the line tension on the arc, dl ($= Rd\theta$), to the applied force, $\sigma b dl$, such that $1/R = 2\sigma/\mu b = 2\sigma b/\tau_o$.

For dynamic equilibrium, the mechanical force, σb, per unit length of the dislocation, the force $-\mu b^2/2R$ due to curvature and the viscous drag force, $-vkT/D_B b$, due to velocity, v, exerted on the pinned dislocation must all sum up to zero, so that

$$\sigma b - \frac{\mu b^2}{2R} - \frac{vkT}{D_B b} = 0$$

The bowed dislocation must therefore move with velocity

$$v = \left(\sigma - \frac{\mu b}{2R}\right)\frac{b^2 D_B}{kT} \tag{8}$$

which has the same form as Einstein's mobility equation.

For material transport by pipe diffusion whereby lattice diffusion is negligible, the climb proceeds entirely by core transport between bubbles and dislocations during the climb–drag process. If the dislocation can adjust its shape quickly compared with the rate at which the bubble is dragged, the dislocation is able to maintain a uniform curvature, $1/R$, which is in equilibrium with the surface tension, γ, and the pressure, p, in the bubble.

For the climb of pinned dislocation, which is controlled by pipe diffusion, all the vacancies that are involved in the climb process must be supplied or removed along the dislocation at the pinning points. This requires that the adjacent dislocation link is able to accept or supply these vacancies. Because the dislocation is part of the three-dimensional network in quartz (Fig. 3), this requirement is satisfied if the orientations of adjacent links with respect to the stress are such that one link acts overall as a vacancy source

and the other as the sink. As the diffusion distance increases, the dislocation becomes more bowed.

The vacancy concentration at a bubble surface is given by the relationship [20]

$$C_b = C_{eq} \exp\left[\left(2\frac{\gamma}{\alpha} - p\right)\frac{b^3}{kT}\right] \quad (9)$$

where C_{eq} is the thermal equilibrium vacancy concentration and $\alpha = \delta/2$ is the bubble radius. The vacancy concentration at the dislocation is given by

$$C_d = C_{eq} \exp\left[\left(\sigma - \frac{\tau}{bR}\right)\frac{b^3}{kT}\right] \quad (10)$$

In steady state conditions, $C_b = C_d$ and hence

$$\frac{1}{R} = \left(\sigma + p - \frac{2\gamma}{\alpha}\right)\frac{b}{\tau} \quad (11)$$

The dislocation climb behaviour by pipe diffusion is determined or controlled by the effect of bubble mobility. For diffusion controlled climb, the bubble mobility can be expressed by the relationship [28]

$$M_B = \left(\frac{b}{\alpha}\right)^4 \frac{D_B}{kT} \quad (12)$$

where D_B is the diffusion coefficient of the bubbles. If the bubbles are of limited mobility, a dislocation can adjust its configuration during the climb process, at a rate that can be rapid in comparison with the rate of bubble drag. The dislocation curvature is then given by Equation 11 and the overall velocity is controlled by the dragging processes, and Equation 8 then represents the drag velocity, v_d.

However, if the bubble is relatively mobile, the dragging process may be sufficiently rapid that the dislocation cannot maintain the dynamic equilibrium configuration defined by Equation 8; and if the drag becomes so rapid, then the equilibrium curvature, $1/R = 2\sigma b/\tau$, cannot be maintained. The dislocation must then adopt a lesser effective curvature, such that the processes of climb and drag occur at matching rates.

2.4. Microcreep

As already observed, a dislocation subjected to a stress too small to free it from pinned bubbles can only be moved by dragging the bubbles along by diffusion, which may lead to slower strain rates resulting in microcreep.

At a temperature, T, large enough for thermal agitation, kT, to be larger than the binding energy, long range elastic interaction between moving dislocations and bubbles at an average distance, λ, in the cloud can be considered. Because $W \approx 10^{-16}\,\text{J} \gg kT$, where $kT \sim 10^{-20}\,\text{J}$, the above assumption cannot hold; rather the bubbles are expected to be at a minimum distance, $\lambda \approx b$, from the dislocation, which can then lead to the observed pinning. It is therefore the drag of these pinning bubbles that contributes to creep deformation.

The dragging contribution to the deformation leads to a microcreep mechanism, and the microcreep rate, $\dot{\varepsilon}_m$, can be deduced from pipe diffusion of a pinned dislocation as illustrated in Fig. 5. When a bubble, G, jumps forwards a distance, b, into position G_1 under the applied stress, σ, the dislocation loop MGN has enough time to move forwards. The subsequent work done by the stress is $\sigma b^2 L$, and the frequency of vibration of this event is

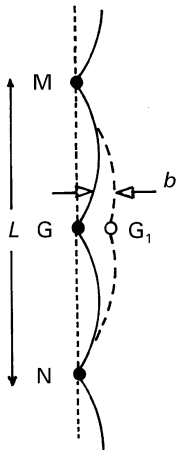

Figure 5 Schematic diagram of microcreep for a dislocation dragging mobile bubble.

$$\nu = \nu_0\left(\frac{b}{L}\right)\exp\left(-\frac{U_B}{kT}\right) = \nu_1 \exp\left(-\frac{U_B}{kT}\right) \quad (13)$$

where $\nu_0(b/L)$ is the frequency of vibration of MGN and U_B is the diffusion energy of the bubble.

Taking into account the forward and backward jumps of the bubbles, the microcreep rate equation can be written as

$$\dot{\varepsilon}_m = \left(\frac{\rho}{L}\right)(b^2 L)\nu_0\left(\frac{b}{L}\right)\left[\exp\left(-\frac{U_B - \sigma b^2 L}{kT}\right) - \exp\left(-\frac{U_B + \sigma b^2 L}{kT}\right)\right]$$

or

$$\dot{\varepsilon}_m = \left(2\rho\frac{b}{L}D_B\right)\sin h\left(\frac{\sigma b^2 L}{kT}\right) \quad (14)$$

where D_B is the diffusion coefficient of the bubble. For quartz single crystals, if $b \sim 6\times10^{-10}\,\text{m}$, $L \sim 5\times10^{-7}\,\text{m}$, $\sigma \sim 3\times10^3\,\text{Pa}$, then $\sigma b^2 L/kT \ll 1$, and hence Equation 14 reduces to

$$\dot{\varepsilon}_m \approx 2\rho D_B \frac{\sigma b^3}{kT} \quad (15)$$

Equation 15 shows that the microcreep rate resulting from dislocation–bubble drag is directly proportional to the applied stress and is independent of the concentration of the bubbles. Hence, the microcreep stress exponent, $n_m = 1$, agrees with the general criteria for diffusion controlled creep.

3. Discussion

The experimental results presented in the previous section demonstrate that bubbles can be formed at dislocations and, that from theoretical considerations,

bubbles can be dragged along by dislocations if the applied stress is low, while for large stress, the dislocations can break free completely.

For the bubble drag mechanism, it has been assumed that the bubbles maintain equilibrium size. But a significant departure from equilibrium conditions is arbitrarily defined to occur when the fluid pressure exceeds twice the surface tension restraining pressure, i.e. $p \geqslant 2\gamma/\alpha$ [29]. If external sources and sinks for vacancies exist, bubbles can achieve an equilibrium condition if $C_b = C_{eq}$ in Equation 9 by emitting vacancies if $2\gamma/\alpha > p$, or by absorbing vacancies if $p > 2\gamma/\alpha$ where the equilibrium radius is defined as $2\gamma/p$. For bubbles spaced less than 0.5 μm apart, it is concluded that sufficient vacancies are available so that $p \approx 2\gamma/\alpha$. Higher excess pressure is also expected when bubbles are more widely spaced; and in cases where p becomes significantly greater than $2\gamma/\alpha$, it is conceivable that bubble growth by dislocation generation can occur.

If there are differences in bubble sizes, then there must be a critical bubble size below which the bubbles have a tendency to remain attached to the dislocations; whereas the larger bubbles, due to their restricted mobility, have a retarding effect [30]. It should be noted that in Figs 1 and 2, the precipitated water bubbles have nearly the same diameter of ~ 40 nm and no clear distinction can therefore be made between any smaller or larger bubbles. The interaction between bubbles and dislocations can then be considered only in terms of the level of applied stress while keeping the size term constant. At higher stress levels, the surface tension force is insufficient to stop the bubble drag movement.

4. Conclusions

1. There are two possible reactions when a dislocation encounters a second phase bubble: the dislocation may be pinned by the bubble or the dislocation may drag the bubble with it. If the driving force for the dislocation motion exceeds the pinning force exerted by the bubble, the dislocation is pulled free of the bubble and sweeps across the lattice.

2. Dislocations pinned by water bubbles can only escape by climb through the pipe diffusion mechanism. If the applied stress is very small, the dislocation can escape by dragging the bubbles, which will lead to a microcreep strain rate proportional to the applied stress.

3. The presence of bubbles slows down the velocity of movement of the dislocations provided the bubbles are attached to the bubbles. The behaviour of precipitates not attached to dislocations may be different, as they remain fixed in the matrix and may either permit local movement of the dislocation or complete dislocation breakaway.

4. Thermal activation alone cannot facilitate dislocation breakaway, and an applied stress is necessary.

Acknowledgements

The author would like to thank the Fulbright Fellowship Board, USA, for sponsorship and Professor T. G. Langdon for provision of research facilities to complete this work at the Department of Materials Science and Engineering, University of Southern California, Los Angeles.

References

1. D. T. GRIGGS and J. D. BLACIC, *Trans. Amer. Geophys. Union* **45** (1964) 102.
2. *Idem Science* **147** (1965) 292.
3. K. H. G. ASHBEE, *Amer. Mineral.* **58** (1973) 947.
4. R. D. BAETA and K. H. G. ASHBEE, *Phil. Mag.* **22** (1969) 601.
5. D. J. MORRISON-SMITH, M. S. PATERSON and B. E. HOBBS, *Tectonophys.* **33** (1976) 43.
6. J. M. CHRISTIE and A. J. ARDELL, in "Electron Microscopy in Mineralogy", edited by H. R. Wenk (Springer Verlag, Berlin, 1976) p. 374.
7. A. AYENSU and K. H. G. ASHBEE, *Phil. Mag.* **36** (1977) 713.
8. S. H. KIRBY and J. W. McCORMICK, *Bull. Mineral.* **102** (1979) 124.
9. K. R. S. S. KEKULAWALA, M. S. PATERSON and J. N. BORLAND, in "Mechanical Behaviour of Crystal Rocks", edited by N. L. Carter, M. Friedman, J. M. Logan and D. W. Steams, Geophysics Monograph 24 (American Geophysics Union, Washington, DC) p. 49.
10. J. D. BLACIC and J. M. CHRISTIE, *J. Geophys. Res.* **89** (1984) 4223.
11. J. C. DOUKHAN and L. TRÉPID, *Bull. Mineral.* **108** (1985) 97.
12. A. AYENSU, *J. Mater. Sci. Lett.* **14** (1995) 106.
13. M. I. HEGGIE and R. JONES. *Phil. Mag. Lett.* **55** (1987) 47.
14. M. I. HEGGIE, R. JONES, C. D. LATHAN, S. C. P. MAYNARD and P. TOLE, *Phil. Mag. B* **65** (1992) 463.
15. M. I. HEGGIE, *Phil. Mag. Lett.* **65** (1992) 155.
16. R. JONES, S. OBERG, M. I. HEGGIE and P. TOLE, *ibid.* **66** (1992) 61.
17. M. I. HEGGIE, *Nature* **355** (1992) 337.
18. P. CORDIER, J. C. DOUKHAN and C. RAMBOZ, *Europ. J. Mineral.* **6** (1994) 745.
19. P. CORDIER and J. C. DOUKHAN, *Phil. Mag. A* **72** (1995) 497.
20. A. GREENWOOD, J. E. FORMAN and D. E. RIMMER, *J. Nuclear Mater.* **4** (1959) 305.
21. B. BURTON, *Phil. Mag. A* **52** (1958) 669.
22. D. T. KNIGHT and B. BURTON, *ibid* **59** (1989) 1027.
23. *Idem*, *ibid.* **66** (1992) 289.
24. A. H. COTTRELL and M. A. JAWSON, *Proc. R. Soc. A* **199** (1994) 104.
25. A. AYENSU and K. H. G. ASHBEE, *Metallog.* **11** (1978) 369.
26. J. FRIEDEL, "Dislocations" (Pergamon Press, Oxford, 1964) p. 389–93.
27. F. R. N. NABARRO, "Theory of Dislocations" (Clarendon Press, Oxford, 1967) p. 349–55.
28. F. A. NICHOLLS, *J. Nuclear Mater.* **30** (1968) 73.
29. M. V. SPEIGHT, *Metal. Sci. J.* **2** (1968) 73.
30. M. V. SPEIGHT and G. W. GREENWOOD, *Phil. Mag.* **9** (1964) 683.

Received 7 June
and accepted 17 July 1996